

## Optical extinction due to intrinsic structural variations of photonic crystals

A. Femius Koenderink,\* Ad Lagendijk,<sup>†</sup> and Willem L. Vos<sup>†</sup>

*Complex Photonic Systems, MESA<sup>+</sup> Institute for Nanotechnology and Department of Science & Technology, University of Twente, P. O. Box 217, 7500 AE Enschede, The Netherlands*

(Received 22 June 2005; revised manuscript received 25 August 2005; published 18 October 2005)

Unavoidable variations in size and position of the building blocks of photonic crystals cause light scattering and extinction of coherent beams. We present a model for both two- and three-dimensional photonic crystals that relates the extinction length to the magnitude of the variations. The predicted lengths agree well with our experiments on high-quality opals and inverse opals, and with literature data analyzed by us. As a result, control over photons is limited to distances up to 50 lattice parameters ( $\sim 15 \mu\text{m}$ ) in state-of-the-art structures, thereby impeding applications that require large photonic crystals, such as proposed optical integrated circuits. Conversely, scattering in photonic crystals may lead to different physics such as Anderson localization and nonclassical diffusion.

DOI: [10.1103/PhysRevB.72.153102](https://doi.org/10.1103/PhysRevB.72.153102)

PACS number(s): 42.70.Qs, 42.25.Dd, 42.25.Fx, 81.05.Zx

The promise of full control over emission and propagation of light has led to a widespread pursuit of photonic crystals in recent years.<sup>1</sup> Photonic crystals are dielectric structures in which the refractive index varies periodically over length scales comparable to the wavelength of light. For three-dimensional periodicities, such crystals promise a photonic band gap, i.e., a frequency range for which emission and propagation of light are completely forbidden. Ideally, photonic-band-gap crystals will form a backbone in which many photonic devices, such as ultrasmall waveguides, cavities, and light sources, are combined to create optical integrated circuits.<sup>2</sup> This requires photonic crystals with negligible optical extinction over millimeter distances.<sup>2</sup>

Tremendous progress has been made in the fabrication of photonic-band-gap materials of the required high-refractive-index materials,<sup>3–6</sup> with low point and plane defect densities.<sup>6</sup> Structural variations in size and position of the building blocks, however, are intrinsic to three- (3D) and two-dimensional (2D) photonic crystals alike, amounting to at least 2–7% of the lattice spacing in all current state-of-the-art photonic crystals.<sup>3,7,8</sup> While displacements are well known in condensed matter,<sup>9</sup> size polydispersity of individual unit cell building blocks, including roughness, is intrinsic to metamaterials such as photonic crystals. All such variations can ultimately be traced back to basic thermodynamic arguments,<sup>9</sup> but are at present probably limited by materials science. These deviations from perfect periodicity cause scattering, and hence exponential attenuation of coherent beams propagating through photonic crystals over lengths  $\ell$ , also known as the “(extinction) mean free path.” After propagating over a distance  $\ell$ , a coherent light beam is converted to a diffuse glow that corrupts the functionality of any photonic integrated circuit. Conversely, short mean free paths open up physics related to diffusion of light and ultimately Anderson localization of light.<sup>10,11</sup> Therefore, it is crucial to obtain the relation between the extinction length  $\ell$  and the structural disorder. In this paper, we derive such a relation and test it against available experimental results.<sup>12</sup>

We consider extinction in photonic crystals due to scattering by size polydispersity and displacements from lattice sites of the structural units (size  $r$ ) that compose the unit cell

(lattice spacing  $a$ ). Light scattering is caused only by the *difference* in refractive-index profile of the displaced, slightly polydisperse building blocks as compared to the ideally ordered structure. As illustrated in Fig. 1, this difference is a collection of thin shells of high- and low-index material. The polydispersity and displacements of the building blocks translate linearly into the shell thickness  $\Delta r$ . Since in many photonic crystals, such as cubic (3D) or hexagonal (2D) structures, light transport is isotropic, we treat the ideal crystal as an effectively homogeneous medium with index  $n_{\text{eff}}$  equal to the volume-averaged refractive index.<sup>13</sup> Within this framework, the inverse extinction length

$$\frac{1}{\ell} = \rho \sigma_{\text{Rayleigh}} F \quad (1)$$

is the product of three factors:<sup>14</sup> Rayleigh’s extinction cross section  $\sigma_{\text{Rayleigh}}$  of each shell, the number density of shells  $\rho$ , and a wavelength-dependent geometrical factor  $F$  which embodies corrections beyond Rayleigh scattering.<sup>15</sup> Since the volume of each shell is proportional to its thickness  $\Delta r$ , Rayleigh’s extinction cross section is proportional to  $(m-1)^2 \Delta r^2$ , where  $m$  is the index contrast relative to the background medium. Even though scattering by each shell is generally weak, the huge density  $\rho$  set by the number of structural units per unit cell causes the scattering mechanism to be important. For Rayleigh scatterers, in the low-frequency limit, the dimensionless factor  $F$  equals unity. For weakly scattering shells, the Rayleigh-Gans approach is suited to find  $F$ .<sup>14,15</sup>

We now focus on the extinction length in 3D photonic crystals that consist of spheres (mean radius  $r$ ), such as opals and inverse opals where many data are available. Size polydispersity results in scattering due to thin spherical shells with a Gaussian distribution of thicknesses. The inverse extinction length  $\ell$  scales quadratically with the size polydispersity  $\Delta r$  and with  $m-1$ , since Rayleigh’s extinction cross section for a shell of thickness  $\Delta r$  reads  $\sigma_{\text{Rayleigh}} = (32\pi/3) \times (m-1)^2 k_{\text{eff}}^4 r^4 \Delta r^2$  (cf. Ref. 14), with  $k_{\text{eff}}$  the wave vector in

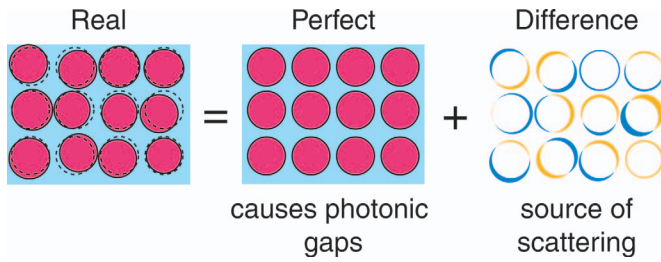


FIG. 1. (Color) (Schematic) Any 2D or 3D real photonic crystal is an ordered stack of building blocks with a spread  $\Delta r$  in their average radius  $r$ , each slightly displaced (displacement  $\Delta u$ ) from the lattice sites. The real structure is the sum of the perfect crystal and the difference between the real and perfect structures. This difference is a collection of thin shells that each scatter weakly. Due to their high number density, the shells dominate the scattering loss.

the effective medium. We find that the Rayleigh-Gans correction<sup>14</sup>

$$F(k_{\text{eff}}r) \approx 0.78 \frac{1}{(k_{\text{eff}}r)^2} (1 + 0.09k_{\text{eff}}r) \quad (2)$$

reduces the well-known fourth-power Rayleigh increase of extinction to a nearly quadratic dependence on wave vector.<sup>16</sup> We have checked the validity of our result using the exact Mie solution for spherical shells. Although for  $m > 2$  and  $k_{\text{eff}}r > 1$  the Rayleigh-Gans result underestimates the extinction loss compared to Mie theory, the Mie model reproduces the quadratic scaling with frequency and shell thickness. Our model captures the effect of both polydispersity  $\Delta r/r$  and displacements  $\Delta u/r$ : calculations of  $F$  show that both effects are similar in magnitude, and can be combined by taking an *effective* shell thickness  $\Delta r + 0.5\Delta u$ . From now on,  $\delta R$  indicates *effective* shell thicknesses normalized by the shell radius. An essential result of our paper is that given the current fabrication accuracies of  $\delta R \sim 5\%$ , the maximum extinction length  $\ell$  is only 50 lattice spacings in high-index crystals at relevant frequencies.

Enhanced backscattering measurements obtained earlier by us have allowed us to determine the mean free path<sup>15</sup>  $\ell$  in synthetic opals, i.e., fcc crystals of close packed polystyrene spheres with  $n=1.59$  and  $n_{\text{eff}}=1.45$ .<sup>17</sup> In Fig. 2(a), we plot  $\ell$  for a wide normalized frequency range, obtained with  $\lambda = 632, 685, \text{ and } 780 \text{ nm}$ , and many different  $a$ . We see that  $\ell$  decreases from  $100a$  for frequencies below first-order diffraction, to  $5a$  at the highest frequencies, where we have converted the wave vector from the scattering model to the frequency scale  $a/\lambda$  typical of photonic crystals. The data and our model agree well on both the observed decrease of  $\ell$  with  $a/\lambda$  and the magnitude of  $\ell$ , which confirms that extinction is due to nonuniformities and displacements of the spheres, assuming  $\delta R = 5\%$ . This value matches well with the cumulative effect of polydispersity  $\sim 2\%$  and rms displacements of spheres from their lattice sites ( $\leq 3.5\%$  of the nearest-neighbor distance), as independently determined by small-angle x-ray scattering.<sup>18</sup> In contrast, the data refute the often assumed Rayleigh  $\omega^4$  dependence.<sup>4,19</sup> The degree of extinction is also inconsistent with the common assumption that scattering is due to point defects, e.g., missing spheres:

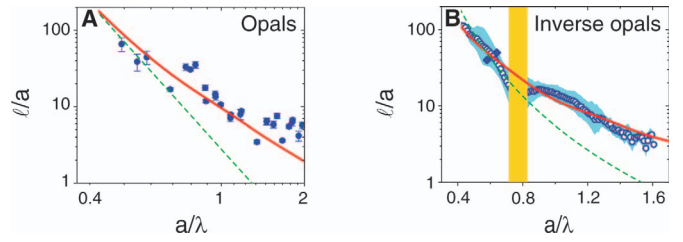


FIG. 2. (Color) Symbols, mean free path (Ref. 15)  $\ell$  in units of  $a$  versus normalized frequency  $a/\lambda$  in polystyrene opals (a) and titania inverse opals (b). Open symbols in (b) were obtained by averaging for each  $a/\lambda$  total transmission spectra for many samples with different  $a$ . The blue shaded area indicates the standard deviation. In the stop gap (orange bar), total transmission is reduced in excess of  $\ell/L$  due to Bragg reflection of the input beam. This affects the data in this limited range. Previous data show that  $\ell$  is unaffected if the frequency is tuned through a gap (Ref. 17). In both (a) and (b), the extinction length agrees well with the model (1) and (2) with  $\delta R \sim 5\%$  (red curves). Green curves represent scaling of  $\ell$  with  $\omega^{-4}$ , and illustrate the failure of Rayleigh scattering models.

From the cross section of a sphere<sup>14</sup> we calculate that the observed scattering would require a density of missing spheres larger than  $0.13a^{-3}$ , an order of magnitude larger than the estimated density<sup>6,19</sup>  $0.01a^{-3}$ .

We have carried out experiments to probe scattering losses in photonic crystals with high photonic interaction strength, i.e., inverse opals in a  $\text{TiO}_2$  backbone. The strength of the interaction of a photonic crystal with light is gauged by the relative bandwidth  $S$  of the lowest order gap in the dispersion relation (see Ref. 1, p. 194). The generally pursued large interaction strengths require a large index contrast  $n_{\text{high}}/n_{\text{low}}$  and are thus associated with stronger scattering, due to the factor  $(m-1)^2$  in Rayleigh's cross section. While the magnitude of the nonuniformities is similar to those in

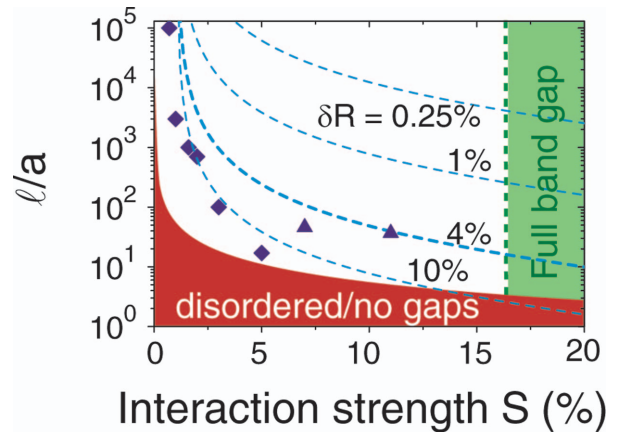


FIG. 3. (Color) Universal dependence of extinction length on interaction strength  $S$  in photonic crystals. Dashed curves, extinction calculated for fcc inverse opals (assuming 26% high-index material). Symbols, our data ( $\blacktriangle$ ), and literature data analyzed by us ( $\blacklozenge$ ). Observed losses are consistent with  $\delta R > 4\%$ . If  $\ell$  is shorter than the length needed for Bragg diffraction, structures are essentially disordered (shaded red). Complete band gaps are expected for  $S > 15\%$  (shaded green). Photonic-crystal integrated circuits require  $\ell/a \geq 10^4$  at  $S > 15\%$ , beyond current state of the art.

TABLE I. Photonic interaction strength  $S$ , structure, and extinction in 3D photonic crystals.

Reference	$S$	$n_{\text{sphere}} (n_{\text{inter}})^{\text{a}}$	$r/a$	$\ell/a^{\text{b}}$	$x_{\text{expt}} (x_{\text{RG}})^{\text{c}}$	$\delta R^{\text{d}}$
22 <sup>e</sup>	0.7%	1.59 (1.33)	0.116 <sup>f</sup>	10 <sup>5</sup>	4 (3.3)	12%
21 <sup>e</sup>	<1%	1.42 (1.48)	cp <sup>g</sup>	3000	3 (2.6)	6%
20 <sup>e</sup>	1.6%	1.59 (1.33)	0.143	1000	3.3 (3)	15%
19 <sup>e</sup>	2%	1.32 (1.47)	cp	700	2.6 (2.6)	6%
24 <sup>e</sup>	3%	1.59 (1.33)	cp	100	$\leq 2$ (2.5)	7%
25 <sup>h</sup>	5%	1.41 (1.0)	cp	17		9%
23 <sup>e, i</sup>	5.5%	1.45 (1.0)	cp		2.6 (2.4)	
Fig. 2(a) <sup>h</sup>	7%	1.59 (1.0)	cp	50	1.8 (2.4)	5%
Fig. 2(b) <sup>i</sup>	11%	1.0 (2.7)	cp	40	2.6 (2.5)	4%

<sup>a</sup> $n_{\text{sphere}} (n_{\text{inter}})$  refractive indices of spheres (background medium).

<sup>b</sup>The  $\ell/a$  are for  $a/\lambda$  in the first stop gap.

<sup>c</sup>Decay powers  $x$  obtained by fitting  $\ell \propto \omega^{-x}$  to the data ( $x_{\text{expt}}$ ) [model Eqs. (1) and (2) in the same frequency range ( $x_{\text{RG}}$ )].

<sup>d</sup>Effective shell radii that best fit the data over the full available frequency range.

<sup>e</sup>Transmission.

<sup>f</sup>bcc instead of fcc.

<sup>g</sup>cp=close packing,  $r/a=1/\sqrt{8}$ .

<sup>h</sup>Enhanced backscattering.

<sup>i</sup>Diffuse total transmission.

the direct opals,<sup>3</sup> the inverse opals present a much larger index contrast  $n=2.7\pm 0.4$  ( $n_{\text{eff}}\approx 1.18$ ). We have determined the frequency dependence of  $\ell$  from total diffuse transmission ( $T=\ell/L$ , with  $L$  the sample thickness<sup>15</sup>). We used white-light Fourier transform spectroscopy to cover a wide normalized frequency range for many samples with  $a=650\text{--}930$  nm. To obtain the absolute magnitudes of the mean free paths we calibrated our measurements by measuring the absolute values of the transmission (closed symbols) and using enhanced-backscattering data.<sup>17</sup> Figure 2(b) shows that  $\ell$  decreases from  $100a$  at  $a/\lambda=0.4$  to only  $4a$  at  $a/\lambda=1.6$ . This decrease of  $\ell$  for the inverse opals is in excellent correspondence with our prediction (solid curve), taking a nonuniformity  $\delta R=4\%$  that is consistent with independent structural data.<sup>3</sup>

To further test the validity of our model, we have analyzed transmission data reported in many papers encompassing fcc and bcc photonic crystals, with sphere volume fractions from  $\varphi=0.7\text{--}74\%$  and index contrasts  $n_{\text{high}}/n_{\text{low}}$  from 1.05 to 1.5.<sup>19–25</sup> Extinction causes the coherent-beam transmission outside stop gaps to decrease according to Lambert-Beer's law  $T_{\text{coh}}=e^{-L/\ell}$ . In all cases, except of course for the dilute crystal,<sup>22</sup> fitting a power-law dependence  $\ell \propto \omega^{-x}$  to each data set shows that extinction does not increase according to Rayleigh's law. Indeed, Table I shows that we find exponents  $x<4$  in reasonable correspondence to the exponents predicted by our model in the same frequency windows. Similar exponents were recently also observed in Ref. 26. Fits to our model further show that extinction lengths for the wide range of crystals agree with  $\delta R>4\%$ , consistent with typical sphere polydispersities and displacements of 2–5%, as reported in Table I. The quantitative agreement of  $\ell$  with Eqs. (1) and (2) confirms that polydispersity and displacements of unit cell building blocks determine scattering loss in 3D photonic crystals.

Given the success of our model, we can now use it to infer the general dependence of the extinction length  $\ell/a$  on the photonic interaction strength  $S$  and the nonuniformity  $\delta R$ . In Fig. 3 we present both  $\ell/a$  and  $S$  that are calculated as a function of index contrast  $(m-1)$ . It is clear that the extinction length decreases both with increasing photonic strength and with increasing structural disorder. We also present the experimental extinction data from Table I for fcc opals and inverse opals, showing again a good agreement with our model with  $\delta R>4\%$ . A photonic band gap requires interaction strengths beyond  $S=0.15$ ; extinction lengths less than 20 lattice spacings are expected at the current level of fabrication accuracy. Ultimately, one hopes to realize photonic crystals that combine many optical functions. Recent technology roadmaps foresee crystals containing  $\sim 10^4$  optical functions per  $\text{mm}^2$  (Ref. 2, p. 245), requiring negligible loss over more than millimeter distances. From the general scaling of extinction with nonuniformity we conclude that applications of photonic-band-gap crystals in circuits require a formidable tenfold increased perfection in statistical fabrication accuracy to  $\delta R<0.25\%$ , or subnanometer precision. Such an improvement is far beyond the current state of the art.<sup>1,2</sup>

Although 3D photonic crystals potentially offer the best platform for photonic crystal functionality, 2D photonic crystals possess many of the desired properties with the advantage of ease of fabrication. While the fabrication methods are radically different, 2D photonic crystals suffer from polydispersity and displacements of their unit cell building blocks analogous to 3D crystals.<sup>7,8</sup> To obtain the scattering losses, we consider 2D crystals of infinitely long cylinders. Now, Rayleigh's cross section per unit length  $\sigma_{\text{Rayleigh}}=(3\pi^2)(m-1)^2 k_{\text{eff}}^3 r^2 \Delta r^2$  of thin cylindrical shells of thickness  $\Delta r$  and radius  $r$  increases with the cube of the optical frequency.<sup>14</sup> In the relevant range of cylinder radii, the Rayleigh-Gans model causes the  $\omega^{-3}$  dependence of  $\ell$  in the Rayleigh limit to be reduced to  $\omega^{-2.2}$  since<sup>16</sup>

$$F(k_{\text{eff}}r) \approx 0.488(k_{\text{eff}}r)^{-0.8}. \quad (3)$$

For a hexagonal lattice of air cylinders in silicon with  $r/a = 0.45$ , typical for macroporous silicon crystals,<sup>27</sup> we find  $\ell \approx 40a$  for frequencies near lowest-order stop gaps, assuming a nonuniformity  $\delta R$  of 5%. A much larger  $\ell$  is required for integrated circuit applications.

Many efforts currently focus on quantifying losses in 2D crystals made from high-index slabs on lower-index cladding layers, for which the nonuniformity  $\delta R$  is around 5%.<sup>1,7,8</sup> Although the guided wave profile normal to the slab is not incorporated in our model, we believe that Eq. (3) yields a reasonable estimate of scattering due to nonuniformity of the air holes in such structures. Similar to 3D, applications that rely on large structures, such as 2D photonic crystal integrated circuits, require a considerable increase in fabrication accuracies beyond the current state of the art.<sup>1,2</sup> These scattering losses add to widely studied out-of-plane scattering that is intrinsic to some 2D crystal designs, even if perfectly fabricated.<sup>28</sup> In contrast to out-of-plane loss, however, statistical variations cannot be reduced by design optimization.

Scattering in photonic crystals opens opportunities to explore new phenomena in multiple scattering of light.<sup>11</sup> Photonic crystals allow unique control over fundamental aspects, such as the transport velocity or anisotropies of light diffusion. A fascinating application is the possibility to localize light, which could serve to enhance nonlinear interactions.<sup>10</sup> According to the usual Ioffe-Regel criterion, Anderson localization occurs when the mean free path is so strongly reduced that its product with the wave vector equals one:  $k\ell \approx 1$ . It has been proposed that in photonic crystals this challenging criterion is relaxed to  $k\ell \approx 1/\sqrt{\rho_s}$ , with  $\rho_s$  the modification of the photonic density of states (DOS) relative to free space.<sup>29</sup> Since the DOS is strongly reduced in photonic gaps, localization of light may even be feasible with the relatively long mean free paths predicted by our model.

We thank Allard Mosk, Peter Lodahl, Philip Russell, and Thomas Krauss for stimulating discussions. This work is part of the research program of the “Stichting voor Fundamenteel Onderzoek der Materie (FOM),” which is financially supported by the “Nederlandse Organisatie voor Wetenschappelijk Onderzoek (NWO).”

\*Present address: FOM Institute for Atomic and Molecular Physics AMOLF, Center for Nanophotonics, Kruislaan 407, 1098 SJ Amsterdam, The Netherlands. Email address: koenderink@amolf.nl; URL: www.photonicbandgaps.com

†Also at FOM Institute for Atomic and Molecular Physics AMOLF, Center for Nanophotonics, Kruislaan 407, 1098 SJ Amsterdam, The Netherlands.

<sup>1</sup>*Photonic Crystals and Light Localization in the 21st Century*, edited by C. M. Soukoulis (Kluwer, Dordrecht, 2001).

<sup>2</sup>S. Noda and T. Baba, *Roadmap on Photonic Crystals* (Kluwer, Boston, 2003).

<sup>3</sup>J. E. G. J. Wijnhoven and W. L. Vos, *Science* **281**, 802 (1998).

<sup>4</sup>A. Blanco *et al.*, *Nature (London)* **405**, 437 (2000).

<sup>5</sup>S. Noda, K. Tomoda, N. Yamamoto, and A. Chutinan, *Science* **289**, 604 (2000).

<sup>6</sup>Y. A. Vlasov, X. Z. Bo, J. C. Sturm, and D. J. Norris, *Nature (London)* **414**, 289 (2001).

<sup>7</sup>T. Baba and N. Fukaya, in *Photonic Crystals and Light Localization in the 21st Century* (Ref. 1), pp. 105–116; M. Notomi, K. Yamada, A. Shinya, J. Takahoshi, and I. Yokohama, *Phys. Rev. Lett.* **87**, 253902 (2001); S. Ogawa, K. Tomoda, and S. Noda, *J. Appl. Phys.* **91**, 513 (2002).

<sup>8</sup>S. J. McNabb, N. Moll, and Y. A. Vlasov, *Opt. Express* **28**, 2927 (2003), as analyzed by D. Gerace and L. C. Andreani, *Opt. Lett.* **29**, 1897 (2004).

<sup>9</sup>N. W. Ashcroft and N. D. Mermin, *Solid State Physics* (Holt, Rinehart, and Winston, New York, 1976), pp. 616–620.

<sup>10</sup>S. John, *Phys. Rev. Lett.* **58**, 2486 (1987).

<sup>11</sup>*Scattering and Localization of Classical Waves in Random Media*, edited by P. Sheng (World Scientific, Singapore, 1990).

<sup>12</sup>A. F. Koenderink and W. L. Vos, *J. Opt. Soc. Am. B* **22**, 1075 (2005).

<sup>13</sup>Interference between scattering and photonic structure is neglected since (I) the extinction lengths appears to be unaffected

when the frequency is tuned through a photonic gap, even when the gaps severely confine the propagation of light (Ref. 17) and (II)  $\ell$  reflects loss averaged over all allowed Bloch modes, which strongly reduces the importance of individual Bloch mode profiles.

<sup>14</sup>H. C. van de Hulst, *Light Scattering by Small Particles* (Dover, New York, 1981).

<sup>15</sup>Anisotropic scattering can be incorporated in  $F$  to obtain the transport mean free path (Ref. 11). The difference is presently not relevant as anisotropy corrections are modest for difference shells originating from displacements.

<sup>16</sup>This approximation for  $F(x)$  holds to within 5% [Eq. (2)] (10% [Eq. (3)]) for  $x > 2$ .

<sup>17</sup>A. F. Koenderink *et al.*, *Phys. Lett. A* **268**, 104 (2000).

<sup>18</sup>M. Megens and W. L. Vos, *Phys. Rev. Lett.* **86**, 4855 (2001).

<sup>19</sup>Y. A. Vlasov, M. A. Kaliteevski, and V. V. Nikolaev, *Phys. Rev. B* **60**, 1555 (1999).

<sup>20</sup>İ. İ. Tarhan and G. H. Watson, *Phys. Rev. Lett.* **76**, 315 (1996).

<sup>21</sup>C. Koerdt, G. L. J. A. Rikken, and E. P. Petrov, *Appl. Phys. Lett.* **82**, 1538 (2003).

<sup>22</sup>R. D. Pradhan, J. A. Bloodgood, and G. H. Watson, *Phys. Rev. B* **55**, 9503 (1997).

<sup>23</sup>H. Míguez *et al.*, *Appl. Phys. Lett.* **71**, 1148 (1997).

<sup>24</sup>S. H. Park, B. Gates, Y. N. Xia, *Adv. Mater. (Weinheim, Ger.)* **11**, 462 (1999).

<sup>25</sup>J. Huang, N. Eradat, M. E. Raikh, Z. V. Vardeny, A. A. Zakhidov, and R. H. Baughman, *Phys. Rev. Lett.* **86**, 4815 (2001).

<sup>26</sup>R. Rengarajan, D. Mittleman, C. Rich, and V. Colvin, *Phys. Rev. E* **71**, 016615 (2005).

<sup>27</sup>R. B. Wehrspohn *et al.*, in *Photonic Crystals and Light Localization in the 21st Century* (Ref. 1), pp. 143–154.

<sup>28</sup>H. Benisty *et al.*, *Appl. Phys. Lett.* **76**, 532 (2000).

<sup>29</sup>K. Busch and S. John, *Phys. Rev. Lett.* **83**, 967 (1999).